

Analysis of 355 nm Nd:YAG laser interaction with patterned flexible circuit substrates

Péter Gordon / Bálint Balogh / Bálint Sinkovics / Zsolt Illyefalvi-Vitéz

Received 2008-07-22

Abstract

This paper describes a new approach in modeling the interaction and ablation mechanisms of 355 nm Nd:YAG laser and polyimide material.

Generating micro-structures by laser micromachining of inhomogeneous patterned flexible substrates is limited because only a rough estimation on etch rate is possible with a specific set of process parameters. In order to exploit the potential of laser micro-machining, i.e. to generate structures in the resolution range of the focal spot diameter ($\sim 10\text{-}20\ \mu\text{m}$), the effect of laser beam needs to be calculated pulse-by-pulse.

The novelty of the model is that it incorporates the main beam properties of a solid-state laser, the structure of the substrate and the accumulated heat caused by successive pulses, while it eliminates the details of molecular processes which are still considered but only by means of experimental constants.

The model also introduces a new conception of ablation threshold as it is defined as a temperature value instead of pulse energy. This allows the calculation of the amount of ablated material by determining the temperature distribution of the processed material after each laser pulse. This way the model can also take the patterned inhomogeneous structure of the substrate into account, thus allowing material processing by lasers at high resolution.

Experimental and simulation results are compared and evaluated to obtain the model constants (like ablation threshold temperature, transformation efficiency of pulse energy into heat etc.) for 355 nm Nd:YAG lasers and polyimide materials and also for the verification of the model.

Keywords

laser ablation · UV Nd:YAG · polyimide processing

Péter Gordon

Bálint Balogh

Bálint Sinkovics

Zsolt Illyefalvi-Vitéz

Department of Electronics Technology, BME, H-1111 Budapest Goldmann Gy. t. 3., building V2, Hungary

1 Introduction

Flexible substrates (polyesters, polyimides, PEN etc.) are widely used in electronic appliances. As sizes are being reduced and reliability aspects obtain distinguished priority exact calculation and control of laser processing can not be neglected any more. A specific and fixed parameter set will not follow the changes in material properties during the laser exposure thus it does not allow high resolution structuring of the substrate.

This paper explains the choice of laser beam source for precise material processing. The paper then presents the basis of the model and our new considerations. Laser beam energy is absorbed by the material, it is transferred to heat by which a volume of material will be ablated. The paper will point out all losses and effects while it highlights those considered dominant in our approach. The paper will also present a rough evaluation of the model by the comparison of simulation and experimental results.

1.1 Motivation of research

The determination of the amount and structure of the ablated material needs a model for coupling the laser pulse energy into the material and distributing the heat within the material. With traditional simulation methods the calculation of real via or kerf profiles with the desired resolution would take up unacceptably long times for industrial applications.

Our aim is:

- to set up a model that eliminates the dynamic contribution of as many side effects as possible, and takes them into account in an experimentally determined constant value at specific processing environments;
- to build a simulation tool on the basis of the above model that can determine the specific etch rate, i.e. the ablation depth (ablation volume) per pulse during the laser structuring process pulse-by-pulse within an acceptable time.

1.2 Considerations of laser source selection

The variety of laser sources used in material processing is rather small. Applications usually designate one specific laser

type. In the past decade UV Nd:YAG lasers, however, are starting to dominate, even though their cost is still relatively high. The 355 nm wavelength is convincing from three aspects.

- First of all focal spot size is determined by wavelength. Theoretically a frequency tripled Nd:YAG laser can have third of the focal spot diameter than that of a fundamental Nd:YAG laser.
- On the other hand radiation in the UV range is better absorbed by flexible substrate materials. A CO₂ laser beam is also well absorbed but its 10,6 μm wavelength results in unacceptable focal spot sizes.
- Third of all a 355 nm photon has already have enough energy to break up the weakest common chemical bonds (e.g. C-H, N-H) thus the ablation process also relies on photochemical mechanisms besides thermal effects and allows smaller HAZ (Heat Affected Zone).

All three aspects highlight the importance of using UV laser beams. Excimer lasers have even shorter wavelengths (even 153 nm) but their usage in our application is not possible mainly because of their special beam properties. As mentioned above, CO₂ lasers are excluded because of their long wavelength, Nd:YAG lasers are excluded because of the low absorbance of their beam in flexible materials [1, 2].

1.3 Former models of ablation

Former studies on UV beam – polymer interaction were carried out with excimer lasers, recent publications also deal with frequency tripled Nd:YAG lasers as these have been commercially available now for almost a decade. Models established with excimer lasers are now subject to validation experimentally outside the operation ranges of excimer lasers and new models are composed especially concentrating on the beam properties of solid state lasers. Even though the wavelength and pulse duration of an excimer can be close to those of a frequency tripled Nd:YAG laser, their pulse repetition frequency (PRF) is limited to a few hundreds per second and the energy distribution in the beam is completely different, too.

Frequency tripled Nd:YAG lasers appeared commercially only in the last decade. Their advantages over excimer lasers are obvious as far as our application is concerned. Direct patterning of polyimides with this laser source is, however still a new field of application and needs its background to be explored. So far only Yung et al. published their theoretical and experimental results on the thermal aspects of this interaction [3–5] The Gaussian beam shape, the effect of other layers of the structure are just some of the factors that were not considered in their work. As features of the structures to be produced are comparable with the spot size of the beam the above issues can not be neglected. Thus our model does respect the Gaussian beam shape, as well as the cumulative heat effect of consecutive shots as result of high (up to 100 kHz) PRF.

One can experience either photo-thermal or photo-chemical effects or even both at the same time [6], while many other side-effects could be considered like plume, plasma formation [7, 8] resulting complex shielding, acoustic waves due to explosion-like processes causing mechanical impact and stress [9], different heat transfer methods, different material properties in function of temperature and state of matter. Our model, however, does not consider these factors at this state of the work. Laser shots are treated as one-time direct energy transfers into the material, no molecular dynamics (MD) level considerations [10] are implemented.

1.4 Illustrative description of our new model approach

The model for determining the etch rate pulse-by-pulse in an inhomogeneous material has the following new considerations:

- Unlike models on excimer laser exposure our model takes the Gaussian distribution of the laser beam into account.
- Unlike models on determining laser ablation mechanisms our model does not incorporate the dynamic effect of e.g. plume formation, acoustic shocks, changes in material properties in the heat affected zone and does not consider processes in molecular dimensions either.
- Our model, however, takes heat accumulation into account as a key issue. This allows us to give a new interpretation of the ablation threshold, i.e. a limit of conditions from which material is removed from the substrate. Instead of calculating with pulse energy threshold (E_{th}) we introduced substrate temperature threshold (T_{th}). T_{th} is another key issue of the model. E_{th} as a constant value by specific laser processing parameters can not consider heat accumulation, while T_{th} is introduced especially for this reason.

Substrate temperature threshold need to be determined of course. This parameter should be characteristic for different materials and non-dependent of pulse repetition frequency (PRF). So far materials have been described by pulse energy threshold, even though it highly depends on PRF.

If T_{th} is given for a substrate material a simulation tool can be developed, also based on the mechanisms described by our model, i.e. the way pulse energy is transformed into heat and the way heat is distributed within the material.

2 Experimental

This paragraph will present the method we developed to determine T_{th} and other important constants of the model in experimental way and how it was evaluated by simulation. We expect the experimental results to be in good correlation with simulation results and not only by their characteristics but also absolute values should be similar. This would validate the approach of our model.

The experiments were carried out by a Coherent AVIA 355-4500 frequency tripled, Q-switched Nd:YAG laser. The laser

has a built – in thermal lens compensation called ThermaTrack. The length of the resonator is optimized at each pumping diode current – PRF pair to obtain the highest output power and best beam quality. This means that the beam diameter and the energy distribution of the beam can be considered independent from the pumping current i.e. the pulse energy.

The deflection of the beam was accomplished by a Razorscan-10 galvo scan head, which uses an F-theta lens with 100 mm focal length. The most important parameters of the laser system are:

- wavelength: 355 nm
- beam diameter at $1/e^2$: 3.5 mm
- max. PRF: 100 kHz
- pulse length: 20-35 ns (depending on PRF and pumping current)
- max. pulse energy: 300 μJ
- min. spot diameter: $\sim 30 \mu\text{m}$

The base material of the test specimens was polyimide (Upilex™) with 25 and 75 μm thicknesses. The optical inspections were accomplished by an Olympus BX-51 optical microscope.

2.1 Step-1: Determining E_{th} at specific substrate temperatures and specific PRF

To determine E_{th} we punched the substrate and calculated the number of pulses needed to completely drill it through at different pulse energies (E_p) and at a specific PRF (50 kHz). Etch rates at different E_p s are given by the quotient of substrate thickness and required pulse numbers. (This method has an increasing error at higher pulse energies.) See measured values at 50 kHz in Fig. 1.

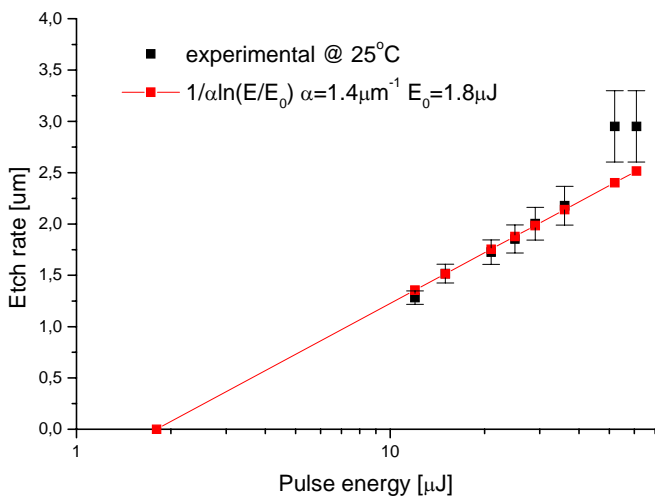


Fig. 1. Measured and calculated etch rate values (errors indicated) and fitted curve at 25°C and 50 kHz PRF

To determine E_{th} from etch rate values the following consideration has been made. The etch rate of excimer lasers is

calculated by:

$$d = \frac{1}{\alpha} \ln \frac{F}{F_{th}} \quad (1)$$

where d is the etch depth per pulse, F is the laser pulse fluence (energy over area) and F_{th} is the ablation threshold fluence [11][12]. The nearly homogeneous energy distribution of excimer lasers explains the use of fluence. The Gaussian energy distribution in the beam of Nd:YAG lasers, however, requires us to replace fluence values by energy values:

$$d = \frac{1}{\alpha} \ln \frac{E_p}{E_{th}} \quad (2)$$

Substituting measured $E_p - d$ pairs into (2) the equation will designate the slope of the fitted curve in Fig. 1 and also deliver E_{th} value at the given PRF rate. The slope value refers to the characteristic absorption coefficient (α) of the substrate material. E_{th} in Fig. 1. is the intersection of the fitted curve and the axis of pulse energy.

2.2 Step-2: Determining the temperature rise of the substrate by one laser pulse

The energy density, fluence distribution of a Gaussian laser beam can be written as:

$$F(x, y, z) = F_0 \cdot e^{-\left(\frac{x^2+y^2}{2\sigma^2} - \alpha \cdot z\right)} \quad (3)$$

where x, y, z are the space coordinates with the origin defined at the centre of the beam and axis z is perpendicular to the surface of the material. The first term in the exponent describes the Gaussian distribution of the laser beam and the second comes from the Lambert-Beer law of absorption. The parameter of width (σ) refers to the definition of the minimal spot diameter:

$$4\sigma = d_{min} 2.44 \frac{f M^2 \lambda}{D} \quad (4)$$

where d_{min} is defined where the intensity drops to $1/e^2$ and f is the focal distance, D is the beam diameter, M^2 is a beam quality parameter which is 1 for the TEM₀₀ Gaussian beam and λ is the wavelength [14].

All effects that decrease the energy of the beam in some way before it is absorbed by the material (e.g. plume formation, reflection etc.) is considered in the coupling-in-efficiency-factor, so we introduced CEF.

Pulse energy is the definite integral of the fluence over the whole surface and it has to be reduced by CEF in our model. F_0 is the fluence at the centre of the beam and it can be calculated from the pulse energy.

$$CEF \cdot E_p = \int_{-\infty}^{\infty} \int_{-\infty}^{\infty} F_0 e^{-\frac{x^2+y^2}{2\sigma^2}} dx dy = F_0 2\pi \sigma^2 \quad (5)$$

$$F_0 = \frac{CEF \cdot E_p}{2\pi \sigma^2} \quad (6)$$

$$F(x, y, z) = \frac{CEF \cdot E_p}{2\pi\sigma^2} \cdot e^{-\left(\frac{x^2+y^2}{2\sigma^2} - \alpha \cdot z\right)} \quad (7)$$

The energy in a finite element of volume (a^3) can be calculated based on (3):

$$E = F \cdot a^2(1 - e^{-\alpha \cdot a}) \quad (8)$$

thus the temperature rise in a finite element of volume (a^3) can be calculated:

$$\Delta T = \frac{TEF \cdot E}{c\rho \cdot a^3} \quad (9)$$

where c is the capacity of heat, ρ is the density and TEF (transformation efficiency factor) is a characteristic value for materials what we introduced to express energy to heat transformation efficiency within the material. Its value is 0 if the ablation process is totally photo-chemical and 1 if the ablation is simply a photo-thermal process. At 355 nm laser ablation of polyimide both phenomena take place and their ratio is not determined. The complete loss of converting the original energy of a laser shot to heat is taken into account as $CEF \cdot TEF$, which is ETF, energy-to-temperature transformation efficiency factor.

If (6) is substituted in (9) the highest temperature rise can be calculated by the following expression:

$$\Delta T_{\max} = \frac{ETF \cdot E_p (1 - e^{-\alpha \cdot a})}{2\pi\sigma^2 c\rho \cdot a} \quad (10)$$

and if a is infinitesimally small it can be written, as:

$$\Delta T_{\max} \underset{a \rightarrow 0}{=} \frac{ETF \cdot E_p \alpha}{2\pi\sigma^2 c\rho} \quad (11)$$

This way we found a relation between the pulse energy and the highest theoretical temperature rise it can cause in the material.

If we also consider that material is ablated above E_{th} we can substitute this value in (11) and get the highest real temperature rise.

$$\Delta T_{\max} = \frac{ETF \cdot E_{th} \alpha}{2\pi\sigma^2 c\rho} \quad (12)$$

The value of ETF is still unknown and needs to be determined as follows.

2.3 Step-3: Determining ETF and T_{th}

The value of temperature threshold is determined by the value of the original substrate temperature (T_{sub}) and the highest possible temperature rise:

$$T_{th} = \frac{ETF \cdot E_{th} \alpha}{2\pi\sigma^2 c\rho} + T_{sub} \quad (13)$$

E_{th} and α can be measured and calculated by the above described experiment and equations while ETF and T_{th} is still unknown.

Our method to determine ETF and T_{th} is to carry out the experiment at different substrate temperatures. Higher initial substrate temperature decreases the energy needed to ablate material (E_{th}) and also decreases ΔT_{\max} , while T_{th} remains the same

as it is a characteristic property of the given material.

$$T_{th} = T_{sub1} + \Delta T_{\max 1}(ETF, E_{th1}) = T_{sub2} + \Delta T_{\max 2}(ETF, E_{th2}) \quad (14)$$

This way the value of ETF will balance the difference of T_{sub} 's and ΔT_{\max} s as these need to be equal.

2.4 Results of the experiments

Etch rate measurement experiments were carried out at three substrate temperature values: 25°C, 110°C and 186°C.

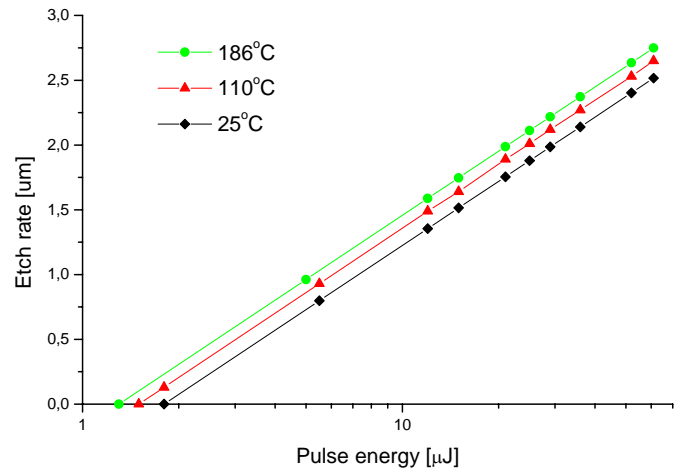


Fig. 2. Ablation rates at different substrate temperatures

Results clearly show our expectations as higher initial substrate temperatures shift the fitted curve to the left thus appointing lower E_{th} values.

If ETF is considered to be 1 the maximal temperature rises are too high and they do not reflect the substrate temperature differences. The 85°C difference between 1.8 and 1.5 µJ E_{th} is observed between ΔT_{\max} values if ETF is 0.132. In this case the ablation threshold temperature (T_{th}) is 535°C, however, it is 554°C at 1.3 µJ. If ETF is 0.176 then the 76°C substrate temperature difference is reflected between the maximal temperature rise values at 1.5 and 1.3 µJ and T_{th} is 677°C in this case.

Based on the result it can be stated that ETF is between 0.132 and 0.176, since in first case the temperature dependency of the etch rate between 25°C and 110°C, in the second case between 110°C and 186°C is presented correctly.

The values of the possible ETF factor and the values of T_{th} present some inaccuracy but they are both in the expected range. Roughly 15% of the beam energy is transferred into heat and the substrate material is ablated when it reaches roughly 600°C.

To validate the above results experiments will also be carried out at different PRFs. Lower PRF means longer times between consecutive shots, so that the heat has more time to disperse in the surrounding zone. This also means that more pulse energy is needed to ablate the material, i.e. E_{th} increases. Temperature threshold value should, however, not change.

Tab. 1. Approximation of ETF based on temperature dependent etch rate measurements

E_{th} μJ	T_{sub} [$^{\circ}C$]	ETF=1		ETF=0.132		ETF=0.176	
		ΔT_{max} [$^{\circ}C$]	T_{th} [$^{\circ}C$]	ΔT_{max} [$^{\circ}C$]	T_{th} [$^{\circ}C$]	ΔT_{max} [$^{\circ}C$]	T_{th} [$^{\circ}C$]
1.8	25	3866	3891	510	535	680	705
1.5	110	3222	3332	425	535	567	677
	(25+ 85)			(510- 85)		(680-113)	
1.3	186	2792	2978	368	554	491	677
	(110+ 76)			(425-57)		(567- 76)	

2.5 Considerations for simulating material processing

The way energy is considered to be transferred to heat has been described above. After the ablation is over the residual heat will dissipate by three modes (conduction, radiation, and transfer). This is how cells in our finite element simulation communicate with each other.

Thermal conduction is described by the Fourier law:

$$q = \lambda \cdot A \cdot gradT \quad (15)$$

where q is the heat flow, λ is the thermal diffusivity, A is the area.

Radiation, according to the Stefan-Boltzmann law is proportional with the fourth magnitude of temperature:

$$q = \varepsilon \cdot \sigma_0 \cdot T^4 \quad (16)$$

where ε is the coefficient of radiation, σ_0 is the black body constant. Heat transfer can be calculated according to the following equation where a_{ht} is the heat transfer coefficient.

$$q = a_{ht} \cdot A \cdot (T_{body} - T_{ambient}) \quad (17)$$

The model equations are applied to describe the thermal processes induced by laser ablation. Our aim is to be able to simulate laser manufacturing processes such as via drilling or large area scanning. To be able to obtain results within a reasonable computation time the processes that occur during the few nanoseconds of the laser pulse duration are not simulated. The laser pulse is considered to transmit its energy in a single time unit. The effects that take place during the ablation process, such as plasma shielding are taken into account only on macroscopic scale and besides heating energy also has photochemical effect, so less than 100% of the pulse energy is turned into heat. This is what we call energy-to-temperature transformation efficiency factor (ETF). The amount of ablated material is calculated so that those material parts are considered to be ablated where the temperature would increase above a certain threshold. This threshold temperature description can qualitatively describe the PRF and substrate temperature dependency of etch rate as it was published in our previous paper [13].

2.6 Simulation results

The simulation tool built on the basis of the above described considerations resulted in many different outputs, these were presented in our previous papers, eg. [15].

Fig. 3 presents an example on the temperature profiles simulated in 75 μm polyimide substrate in the center line of the beam path. The curves after a specific number of applied laser pulses (13 μJ) clearly show the result of ablation as they begin deeper and deeper in the material. The selected curves shown in Fig. 3 represent the temperature profile just before the next laser shot.

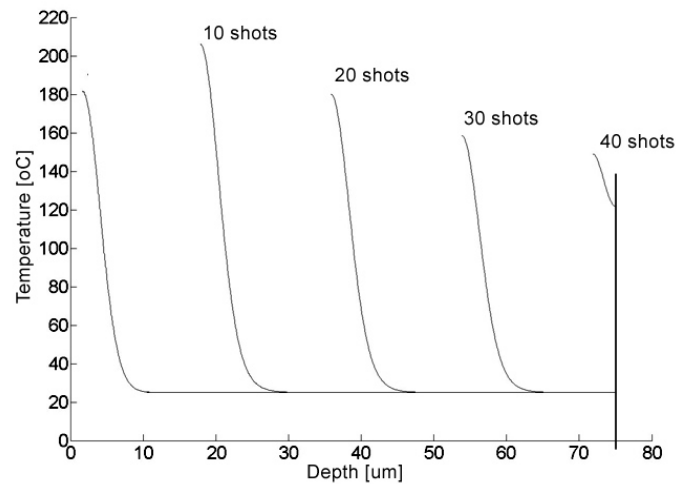


Fig. 3. Temperature profile curves in 75 μm thick polyimide at 50 kHz, 13 μJ laser pulses

Fig. 4 shows simulated surface profiles after consecutive shots, material above the curves is ablated.

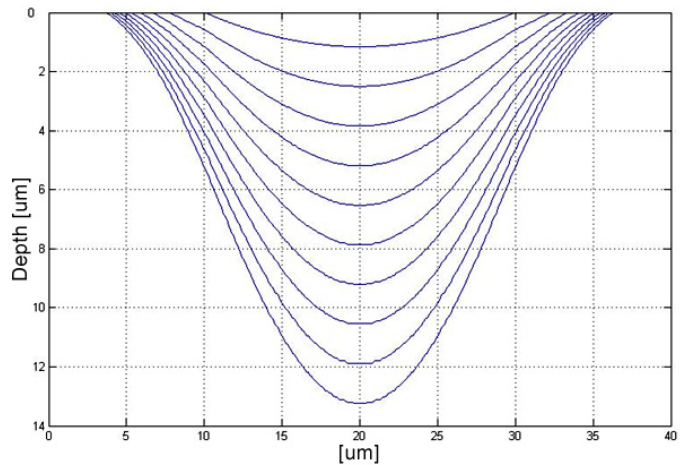


Fig. 4. Simulated surface profiles pulse-by-pulse at 50 kHz, 10 μJ laser pulses

The profiles provided by the simulation that has been based on our temperature threshold model and other considerations de-

scribed above clearly reproduce the characteristic profiles measured in real experiments and absolute values of etched volumes are also in accordance with simulation results.

Simulation methods are also being optimized for an acceptable operation speed and accuracy but reviewing these issues is not subject of this paper.

3 Discussion

The former models mainly concentrated on excimer laser processing of materials and these could not be adapted to our application, so we created a new model for the determination and calculation of ablated volumes.

It has been explained that heat accumulation should not be neglected but the commonly used energy threshold concept can not take this into account. We introduced a new idea of ablation threshold, i.e. to consider the threshold as a temperature value. Material is etched when its temperature is above this value.

A method for determining the temperature threshold value of a specific material has been presented.

Energy threshold values at different substrate temperatures were determined by carrying our etch rate measurements and by a new interpretation of etch rate calculation equation used in excimer laser practice.

Taking into account the Gaussian energy distribution of Nd:YAG laser beams and the exponential absorption of materials an equation has been given for the determination of the highest temperature rise caused by a single laser shot with a specific amount of energy. We also introduced a constant (ETF) which is characteristic to the material and to the processing environment to express all losses of energy before it can be transformed into heat that actually rises the temperature of the substrate. This constant also incorporates the rate of photo-chemical and photo-thermal mechanisms.

A procedure has been presented to determine the above constant and finally our main subject of interest, i.e. the value of temperature threshold.

A simulation tool has been developed to conclude all our considerations. The input of the simulation are the actual structure of the substrate, its temperature threshold value and other characteristic values determined experimentally. At the moment the output of the simulation is the final surface profile (structure) of the material as a result of laser micro-machining with given beam and process parameters.

Even though our simulation tool is still not prepared for the automatic design of a pulse-by-pulse processing procedure to generate a desired micro-structure in a given material, but its current state can already validate our model. As simulation results adequately harmonize with the measurements on a specific material (polyimide) and processing environment set we can state that the model considerations are justifiable. Other flexible materials with other processing parameters will also be processed and measured and also simulated to completely confirm our model.

4 Conclusion

Our work contributed to the researches on polymer ablation with 355 nm Nd:YAG lasers with the following new, main issues:

- Heat accumulation (and Gaussian beam profile) need to be taken into account.
- Temperature threshold (T_{th}) has been introduced and explained instead of energy threshold. Etch rate calculation has earned a new interpretation for Gaussian beams (2).
- Energy-to-Temperature transformation efficiency Factor (ETF) has been introduced to represent all mechanisms that decrease the effective utilization of pulse energy with one empirical constant.
- An equation has been set for the calculation of the highest temperature rise by a single laser shot (12).
- An experimental method has been worked out to determine all constants of the model for a given material and given processing environment.
- A simulation tool has been developed to validate the above considerations.

The results obtained from the simulation promisingly correlate with measured values. At this stage more experiments are being carried out to fine tune our model constants and further development/optimization of the simulation tool is being performed.

References

- 1 **Illyefalvi-Vitéz Zs**, *Laser Processing for microelectronics packaging applications*, Microelectronics Reliability **41** (2001), 563-570, DOI 10.1016/S0026-2714(00)00250-X.
- 2 **Balogh B, Gordon P, Berényi R, Illyefalvi-Vitéz Zs**, *Effect of Patterned Copper Layer on Selective Polymer Removal by 355 nm Laser*, Polytronic 2004, Portland, Oregon, USA, 2004.
- 3 **Yung K C, Liu J S, Man H C, Yue T M**, *355 nm Nd:YAG laser ablation of polyimide and its thermal effect*, Journal of Materials Processing Technology **101** (2000), 306-311, DOI 10.1016/S0924-0136(00)00467-2.
- 4 **Yung K C, Zeng D W, Yue T M**, *XPS investigation of Upilex-S polyimide ablated by 355 nm Nd:YAG laser irradiation*, Applied Surface Science **173** (2001), 193-202, DOI 10.1016/S0169-4332(00)00884-9.
- 5 ———, *High repetition rate effect on the chemical characteristics and composition of Upilex-S polyimide ablated by a UV Nd:YAG laser*, Surface and Coatings Technology **160** (2002), 1-6, DOI 10.1016/S0257-8972(02)00384-5.
- 6 **Illy E K, Brown D J W, Withford M J, Piper J A**, *Enhanced Polymer Ablation Rates Using High-Repetition-Rate Ultraviolet Lasers*, IEEE J.Select. Topics Quantum Electron, posted on 1999, 1543-1548, DOI 10.1109/2944.814996, (to appear in print).
- 7 **Misra A, Mitra A, Thareja R K**, *Diagnostics of laser ablated plasmas using fast photography*, Applied Physics Letter **74** (1999), no. 7, 929-931, DOI 10.1063/1.123412.
- 8 **Bogaerts A, Chen Z, Gijbels R, Vertes A**, *Laser ablation for analytical sampling: what can we learn from modeling*, Spectrochimica Acta Part B **58** (2003), 1867-1893, DOI 10.1016/j.sab.2003.08.004.

- 9 **von Allmen M, Blatter A**, *Laser-Beam Interactions with Materials*, Springer, Berlin, 1998. 2nd. editon.
- 10 **Zhigilei L V, Garrison B J**, *Mechanisms of laser ablation from molecular dynamics simulations: dependence on the initial temperature and pulse duration*, *Appl. Phys. A* **69** (1999), 75-80, DOI 10.1007/s003390051358.
- 11 **Burns F C, Cain S R**, *The effect of pulse repetition rate on laser ablation of polyimide and polymethylmethacrylate-based polymers*, *J. Phys. D: Appl. Phys.* **29** (1996), 1349-1355, DOI 10.1088/0022-3727/29/5/034.
- 12 **Chen Y H, Zheng H Y, Tam S C**, *Excimer laser drilling of polymers*, *Proc of Microelectronics Packaging and Laser Processing*, SPIE, June 23, 1997, pp. 202-210.
- 13 **Balogh B, Gordon P, Sinkovics B**, *Simulation and Indirect Measurement of Temperature Change in Polyimide Induced by Laser Ablation at 355 nm*, *ISSE 2005*, Wiener Neustadt, Austria, 2005, pp. 412-416.
- 14 **William M. Steen**, *Laser Material Processing*, Springer Verlag, 1998.
- 15 **Gordon P, Balogh B, Sinkovics B**, *Thermal simulation of UV laser ablation of polyimide*, *Microelectronics Reliability* **47** (2007), 347-353, DOI 10.1016/j.microrel.2006.01.013.